arXiv:1111.0791v2 [cond-mat.mes-hall] 17 May 2012

Entanglement and Subsystem Particle Numbers in Free Fermion Systems

Y. F. Zhang[1], Huichao Li[1], L. Sheng[1],* R. Shen[1], and D. Y. Xing[1]
[1]*National Laboratory of Solid State Microstructures and Department of Physics, Nanjing University, Nanjing 210093, China*

(Dated: May 18, 2012)

We study the relationship between bipartite entanglement and subsystem particle number in a half-filled free fermion system. It is proposed that the spin-projected particle numbers can distinguish the quantum spin Hall state from other states, and be linked to the topological invariant of the system. It is also shown that the subsystem particle number fluctuation displays behavior very similar to the entanglement entropy. It provides a lower-bound estimation for the entanglement entropy, which can be measured experimentally.

PACS numbers: 73.22.Pr, 03.65.Vf, 03.65.Ud, 65.40.gd, 05.40.Ca

I. INTRODUCTION

Topological phases of matter are usually distinguished by using some global topological properties, such as topological invariants and topologically protected gapless edge modes, rather than certain local order parameters. The integer quantum Hall effect[1], fractional quantum Hall effect[2], and band Chern insulators[3] can be characterized by Chern numbers or Berry phases[4]. The quantum spin Hall (QSH) effect[5,6] and the three-dimensional topological insulators[7,8] are characterized by the Z_2 invariant[9] or spin Chern number[10,11]. Recently, quantum entanglement[12], which reveals the phase information of the quantum-mechanical ground-state wavefunction, has been used as a tool to characterize the topological phases. As shown by Levin and Wen[13] and also by Kitaev and Preskill[14], the existence of topological entanglement entropy in a fully gapped system, such as fractional quantum Hall and the gapped integer spin systems[15,16], indicates existence of long-range quantum entanglement (topological order[17] in equivalent parlance). Another important progress is the demonstration that the entanglement spectrum (ES)[18] reveals the gapless edge spectrum for fractional quantum Hall systems, Chern insulators, and topological insulators[18,20,21].

Supposing A and B to be two blocks of a large system in a pure quantum state, the reduced density matrix (RDM) ρ_A can be obtained by tracing over degrees of freedom of B. Then the Von Neumann entanglement entropy (EE) can be computed

$$S_{ent} = -\mathrm{tr}(\rho_A \ln \rho_A) = -\mathrm{tr}(\rho_B \ln \rho_B) \ . \qquad (1)$$

It has been shown that for bipartite subsystems A and B with a smooth boundary, S_{ent} has the form of $S_{ent} = \alpha L - S_{top}$, where L is the length of the boundary, α is a non universal coefficient, and $-S_{top}$ is a universal constant called the *topological entanglement entropy*[13,14]. Moreover, if we write the RDM in the form of $\rho_A = \exp(-H_{ent})/Z$, where Z is a normalization constant, and H_{ent} is known as the *entanglement Hamiltonian*, the eigenvalue spectrum $\{\varepsilon_i\}$ of H_{ent} is called the ES, which stores more information about the quantum entanglement than the EE[18].

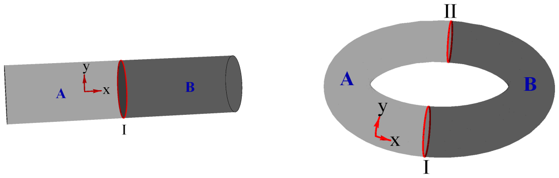

(a) cylinder geometry (b) torus geometry

FIG. 1: (Color online) Schematic view of a cylinder and a torus. The entanglement cuts divide the system into two equal parts A and B. For the cylinder geometry, the entanglement cut leads to one interface (a); and for the torus geometry, the cuts lead to two interfaces (b).

In this paper, we study the relationship between bipartite entanglement and subsystem particle number in half-filled free fermion systems. It was proposed in Ref.[19], for systems with translational invariance in one dimension, the discontinuity in the subsystem particle number as a function of the conserved momentum indicates whether or not the ES has a spectral flow, which is determined by the topological invariant of the system[21]. Nevertheless, this approach has an exceptional case for a half-filled QSH system with two-dimensional inversion symmetry. To overcome the inadequacy, we define spin-projected particle numbers, based on which spin trace indices can be well defined, for the QSH system with or without s_z conservation. Spin trace indices are univocally related to the topological invariant of QSH system, i.e., the Z_2 index. We further investigate the relationship between the EE and subsystem particle number fluctuation. The latter is also dominated by the boundary excitations of the system, and satisfies a similar area law as the EE. It gives a lower-bound estimation of the EE, and can be measured experimentally.

In the next section, we introduce the model Hamiltonian, and explain the procedure to calculate the ES and EE. In Sec. III, numerical calculation of the ES is carried out, and the connection between the subsystem spin-projected particle numbers and the topological invariants in different phases is established. In Sec. IV, the relationship between the EE and subsystem particle number fluctuation is discussed. The final section is a summary.

II. MODEL HAMILTONIAN

We begin with the tight-binding model Hamiltonian for the QSH system introduced by Kane and Mele[5,9], plus an additional exchange field[22]

$$\begin{aligned} H = &-\sum_{\langle \boldsymbol{i},\boldsymbol{j}\rangle} c_{\boldsymbol{i}}^{\dagger} c_{\boldsymbol{j}} + i v_{so} \sum_{\langle\!\langle \boldsymbol{i},\boldsymbol{j}\rangle\!\rangle} c_{\boldsymbol{i}}^{\dagger} \sigma_z v_{ij} c_{\boldsymbol{j}} \\ &+ i v_r \sum_{\langle \boldsymbol{i},\boldsymbol{j}\rangle} c_{\boldsymbol{i}}^{\dagger} (\boldsymbol{\sigma} \times \boldsymbol{d}_{\boldsymbol{ij}})_z c_{\boldsymbol{j}} + \sum_{\boldsymbol{i}} m_i c_{\boldsymbol{i}}^{\dagger} c_{\boldsymbol{i}} + g \sum_{\boldsymbol{i}} c_{\boldsymbol{i}}^{\dagger} \sigma_z c_{\boldsymbol{i}} \ . \end{aligned} \tag{2}$$

Here, the first term is the usual nearest neighbor hopping term with $c_{\boldsymbol{i}}^{\dagger} = (c_{\boldsymbol{i},\uparrow}^{\dagger}, c_{\boldsymbol{i},\downarrow}^{\dagger})$ as the electron creation operator on site $\boldsymbol{i}$, where the hopping integral is set to be unity. The second term is the intrinsic spin-orbit coupling (SOC) with $v_{ij} = (\boldsymbol{d}_{kj} \times \boldsymbol{d}_{ik})_z / |(\boldsymbol{d}_{kj} \times \boldsymbol{d}_{ik})_z|$, where $\boldsymbol{k}$ is the common nearest neighbor of $\boldsymbol{i}$ and $\boldsymbol{j}$, and vector $\boldsymbol{d}_{ik}$ points from $\boldsymbol{k}$ to $\boldsymbol{i}$. The third term stands for the Rashba SOC with $\boldsymbol{\sigma}$ the Pauli matrix. The fourth term stands for a staggered sublattice potential ($m_i = \pm m$), and the last term represents a uniform exchange field with strength g.

We consider systems with cylinder or torus boundary conditions, consisting of N_x (N_x to be even) zigzag chains along the circumferential direction (y direction). The size of the sample will be denoted as $N = N_x \times N_y$ with N_y as the number of atomic sites on each chain. We perform the entanglement cut along the y direction, which results in one or two interfaces between the two equal parts A and B, respectively, for the cylinder or torus geometry, as shown in Fig. 1. In order to examine the EE and ES, an Schmidt decomposition on the ground-state wavefunction or calculation of the RDM is usually needed. For non-interacting fermion systems, however, the necessary information of the entanglement can also be obtained from the following two-point correlators[23]

$$c_{\tau_1,\tau_2}(\boldsymbol{i},\boldsymbol{j}) = \langle c_{\boldsymbol{i},\tau_1}^{\dagger} c_{\boldsymbol{j},\tau_2} \rangle \ . \tag{3}$$

Here, $\langle \cdot \rangle$ means the ground-state expectation of an operator. τ can be an index of spin, pseudospin, or orbital degree of freedom.

Using the Fourier transformation (FT) along the y direction, the Hamiltonian can be rewritten as $H = \sum_{k_y,i,j} c_i^{\dagger}(k_y) h_{i,j}(k_y) c_j(ky)$, where $c_i^{\dagger}(k_y) = (c_{i,\uparrow}^{\dagger}(k_y), c_{i,\downarrow}^{\dagger}(k_y))$ are the electron creation operators. After performing the entanglement cut, we treat part A as the subsystem, and trace out the degrees of freedom of B. It should be noted that any of the correlators $c_{\tau_1,\tau_2}(\boldsymbol{i},\boldsymbol{j})$ with $\boldsymbol{i}$ and $\boldsymbol{j}$ confined in A is unchanged by the tracing. When carrying out the FT on the correlators, we can get

$$c_{\tau_1,\tau_2}(\boldsymbol{i},\boldsymbol{j}) = \frac{1}{N_y} \sum_{k_y} e^{i k_y \cdot (i_y - j_y)} \langle c_{i,\tau_1}^{\dagger}(k_y) c_{j,\tau_2}(k_y) \rangle \ , \tag{4}$$

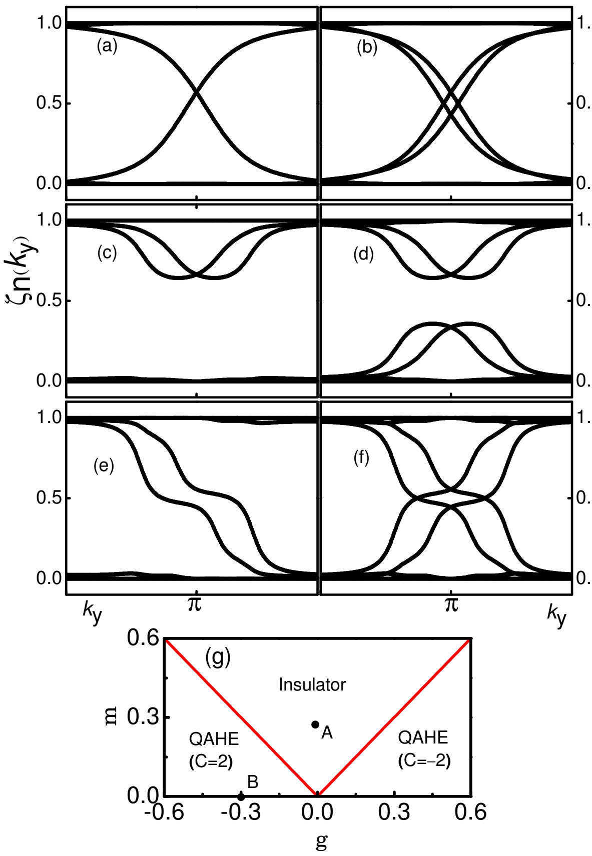

FIG. 2: (a-c) Entanglement spectrum in the cylinder geometry (left panels) and torus geometry (right panels) for the QSH phase with $v_{so} = m = 0.2$, $v_r = 0.1$, $g = 0$ (upper row), the insulator phase with $v_r = -0.3$, $m = 0.3$, $v_{so} = g = 0$ (middle row), and the quantum anomalous Hall phase with $v_r = g = -0.3$, $v_{so} = m = 0$ (lower row). (g) Phase diagram in the m versus g plane for $v_{so} = 0$ and $v_r \neq 0$. Points A and B correspond to the parameter values used (c,d) and (e,f), respectively.

where i and j discriminate the zigzag chains. We use $\langle c_{i,\tau_1}^{\dagger}(k_y) c_{j,\tau_2}(k_y) \rangle$ to form a hermitian matrix $\mathcal{C}(k_y)$. Then the entanglement Hamiltonian is given by [23]

$$H_{ent} = \ln(\mathcal{C}^{-1} - 1) \ . \tag{5}$$

The spectrum $\{\zeta_i\}$ of $\mathcal{C}$ is related to spectrum $\{\varepsilon_i\}$ of H_{ent} by $\zeta_i = 1/(e^{\varepsilon_i} + 1)$, where ζ_i acts as the average fermion number in the entanglement energy level ε_i at "temperature" $T = 1$. By using the spectrum of $\mathcal{C}$, the EE at each k_y sector is given by $s_{ent}(k_y) = \sum_i s_i$, with

$$s_i = -\zeta_i \ln \zeta_i - (1 - \zeta_i) \ln(1 - \zeta_i) \ . \tag{6}$$

From the viewpoint of probability theory, s_i in Eq. (6) can be regarded as the Shannon (information) entropy of the Bernoulli distribution, i.e., the i-th entanglement level ε_i has probability ζ_i of being occupied while $(1-\zeta_i)$ of being unoccupied. As a result, S_{ent} is the Shannon entropy of a series of such independent Bernoulli distributions. In the following, we will perform systematic numerical simulations to study various phases of Hamiltonian (2) in terms of the ES and the subsystem particle number.

III. ENTANGLEMENT SPECTRUM AND SUBSYSTEM PARTICLE NUMBER

At $g = 0$, Hamiltonian (2) is the standard Kane-Mele model[5], which is invariant under time reversal symmetry. The system is in a QSH phase when $|m/v_{so}| < [9 - \frac{3}{4}(v_r/v_{so})^2]$, and is an insulator when $|m/v_{so}| > [9 - \frac{3}{4}(v_r/v_{so})^2]$. On the other hand, if we set $v_{so} = 0$, v_r and g nonzero, a middle band gap opens when $|g| \neq |m|$. The system is in a quantum anomalous Hall phase with Chern number $C = \pm 2$[22] for $|g| < |m|$, and is an insulator for $|g| > |m|$. The band gap closes at the transition point $|g| = |m|$. The phase diagram for $v_{so} = 0$ and $v_r \neq 0$ is plotted in Fig. 2(g).

Figs. 2(a) and (b) show the ES for the QSH phase, Figs. 2(c) and (d) for the insulator phase, and Figs. 2(e) and (f) for the quantum anomalous Hall phase. Here, it should be emphasized that the nontrivial topological phases exhibit gapless ES [Figs. 2(a), (b), (e), and (f)], corresponding to physical gapless edge modes, and this property is named as the *spectral flow*[21]. However, the spectral flow is broken for the topologically trivial phase [Figs. 2(c) and (d)], which is also consistent with the property of the correspondent edge states.

In a recent work[19], the authors proposed a new characteristic quantity called the "trace index" to describe topological invariants, which is defined through a subsystem particle number operator $N_A(k_y) = \sum_{i\in A} c^\dagger_{i,k_y} c_{i,k_y}$. The expectation of $N_A(k_y)$ is given by

$$\langle N_A(k_y)\rangle = \langle GS|\sum_{i\in A} c^\dagger_i(k_y) c_i(k_y)|GS\rangle = \mathrm{Tr}\mathcal{C} \ . \qquad (7)$$

In Fig. 3, we plot the expectation of $N_A(k_y)$ for the three different phases mentioned above. In the cylinder geometry, $N_A(k_y)$ is discontinuous at some discrete momenta in the nontrivial topological phases, as shown in Figs. 3(a) and (c). This is in contrast to the normal insulator phase [see Fig. 3(b)], where $N_A(k_y)$ is a continuous function of k_y. In the torus geometry, $N_A(k_y)$ is exactly equal to half of the total particle number in the k_y sector, without showing any discontinuity, because the change of the particle number in A around interface I is just canceled by that around interface II due to the rotation invariance of the torus. In the cylinder geometry, the *trace index* was defined as the total discontinuities of $\langle N_A(k_y)\rangle$ with varying momentum. Alexandradinata, Hughes, and Bernevig[19] presented a detailed analysis and proved that the trace index is equivalent to the Chern number (or Z_2 invariant) for the Chern (Z_2) insulators. Therefore, the subsystem particle number provides a new alternative tool to reveal the topological invariants.

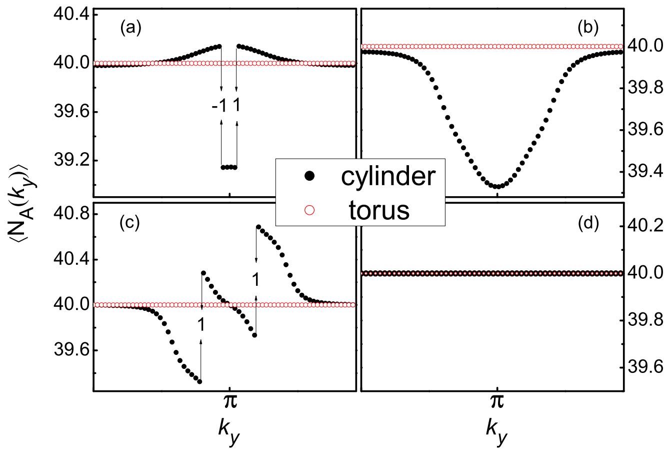

FIG. 3: (Color online) The subsystem particle number in the cylinder geometry and torus geometry for the QSH phase (a), the insulator phase (b), and the quantum anomalous Hall phase (c) with all the parameters same as those in Fig. 2. (d) is also for the QSH phase with $v_{so} = v_r = 0.2$, where the two-dimensional inversion symmetry is retained. Discontinuities in the expectation of the particle number can be observed only in the cylinder geometry.

However, as mentioned in Ref.[19], there is an exceptional case in which the subspace of the occupied bands at the symmetric momenta is not closed under time reversal in the ground state. If at the symmetric momenta the Kramers' doublet that extends along the edge of A is singly-occupied, $\langle N_A(k_y)\rangle$ is continuous, even when the system is in a nontrivial topological phase. For the half-filled system under consideration, an exception still happens. While the two-dimensional inversion symmetry remains unchanged ($m = 0$), $N_A(k_y)$ becomes continuous, as shown in Fig. 3(d). This is because the Kramers' partners extending along the edge simultaneously cross the Fermi level at the symmetric momentum ($k_y = \pi$) and have opposite contributions to the discontinuities of $\langle N_A(k_y)\rangle$.

To overcome this difficulty, enlightened by the definition of the spin Chern number[11], we define spin trace indices. Considering that s_z is not necessarily conserved, it is an adaptable way that we choose operator Ps_zP to split the fiber bundle of the occupied states into two bundles with nontrivial Chern numbers, where P is the ground state projector. At half filling and in the presence of time reversal symmetry ($g = 0$), Ps_zP is always a time-odd operator ($TPs_zPT^{-1} = -Ps_zP$), so that the spectrum of Ps_zP is symmetric in respect to the origin. As a result, the spectral spaces of Ps_zP can provide a splitting of the Hilbert space spanned by the wave functions of the occupied states, resulting in a smooth decomposition $P(k_y)$ into

$$P(k_y) = P^+(k_y) \oplus P^-(k_y) \ , \qquad (8)$$

with $\alpha = \pm$ corresponding to the positive and negative sectors of the spectrum of Ps_zP for all $k_y \in (0, 2\pi]$. Straightforwardly, the two-point correlator matrix can

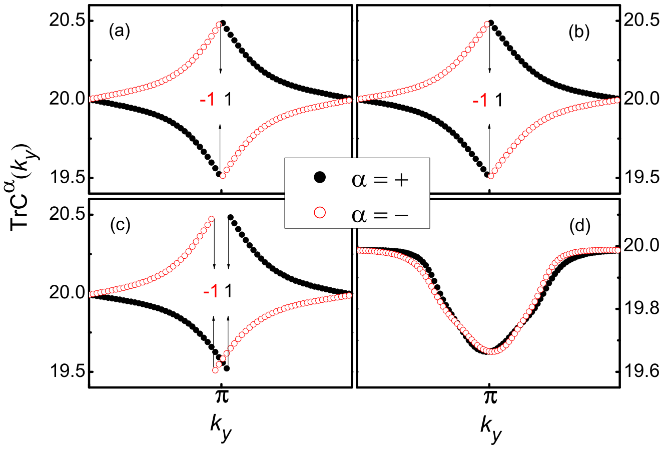

FIG. 4: (Color online) Subsystem spin-projected particle numbers in the cylinder geometry for the QSH phase (a-c) with $g = 0$ and different parameters: (a) $v_{so} = 0.2$ and $v_r = m = 0$, (b) $v_{so} = v_r = 0.2$ and $m = 0$, (c) $v_{so} = m = 0.2$ and $v_r = 0.1$, and for the insulator phase (d) with $v_{so} = v_r = 0.05$, $m = 0.5$ and $g = 0$.

also be decomposed into $\mathcal{C}(k_y) = \mathcal{C}^+(k_y) \oplus \mathcal{C}^-(k_y)$. In this way, the Chern numbers $C_\pm$ of the two spin sectors can be well defined on these new wave functions. It has been proved that $C_\pm$ are topological invariants protected by the energy and spin spectrum gaps[11]. It will be shown below that the traces of $\mathcal{C}^\pm$, called the *spin-projected subsystem particle numbers*, are related to the topological invariants. We plot $\mathrm{Tr}\mathcal{C}^\alpha$ ($\alpha = \pm$) as functions of k_y in Fig. 4. Both $\mathrm{Tr}\mathcal{C}^\alpha(k_y)$ are discontinuous in the QSH phase [Figs. 4(a-c)], in contrast to the continuous functions in the normal insulator phase [Fig. 4(d)]. If $\mathrm{Tr}\mathcal{C}^\alpha(k_y)$ is discontinuous at some discrete momenta $\{k_{dis}\}$ with $k_{dis} \in (0, 2\pi]$, we can define the *spin trace indices* as the total discontinuity, i.e., difference between the limits of $\mathrm{Tr}\mathcal{C}^\alpha(k_y)$ from right and left,

$$A^\alpha \equiv \sum_{k_{dis}} \Big(\lim_{k \to k_{dis+}} \mathrm{Tr}\mathcal{C}^\alpha(k) - \lim_{k \to k_{dis-}} \mathrm{Tr}\mathcal{C}^\alpha(k) \Big) \ , \qquad (9)$$

in the thermodynamic limit. As shown in Figs. 4(a) and (b), no matter whether s_z is conserved, both $\mathrm{Tr}\mathcal{C}^+(k_y)$ and $\mathrm{Tr}\mathcal{C}^-(k_y)$ show discontinuities at momentum $k_y = \pi$ with $A^+ = 1$ and $A^- = -1$ in the QSH phase, where the two-dimensional inversion symmetry is present ($m = 0$). Figure 4(c) shows the discontinuities of $\mathrm{Tr}\mathcal{C}^+(k_y)$ and $\mathrm{Tr}\mathcal{C}^-(k_y)$ in the QSH phase in which s_z is not conserved ($v_r \neq 0$) and the two-dimensional inversion symmetry is broken ($m \neq 0$). In this case, the spin trace indices are equal to 1 and -1, respectively, contributed by two different momentum points. It is noteworthy that in analogy with the Laughlin gauge experiment, A^α can be regarded as the number of particles with spin α pumped from one edge to the other when a unit flux is inserted adiabatically, and so A^α is equivalent to the Chern numbers C_α.

On the other hand, the Z_2 index can be defined as the parity of A^α,

$$A_{Z_2} \equiv A^\alpha mod\ 2, \qquad (10)$$

for any α. As shown in Figs. 4, $A_{Z_2} = 1$ for QSH phase [Figs. 4(a-c)] and $A_{Z_2} = 0$ for insulator phase [Figs. 4(d)]. Therefore, the subsystem particle number expectation can be used to characterize the topological invariants. Especially, for the QSH systems, the spin trace indices are well-defined quantities that can reveal the Z_2 invariant and distinguish different quantum phases.

IV. ENTANGLEMENT ENTROPY AND SUBSYSTEM PARTICLE NUMBER FLUCTUATION

We have shown that topological properties of the ground state can be extracted from the expectation of subsystem particle number. Now we turn to the variance of $N_A(k_y)$. In the past two years, extensive works have been devoted to the study of the relation between the EE and subsystem particle fluctuation for non-topological systems[25]. In this section, we will show that the relation is rather general, it does apply to non-interacting electron systems with a nontrivial band topology. We start from the definition of the variance

$$\triangle N_A^2(k_y) = \langle N_A^2(k_y) \rangle - \langle N_A(k_y) \rangle^2 \ . \qquad (11)$$

Substituting Eq. (7) into Eq. (11) and using the Wick's theorem to expand all the four-point correlators, one can obtain

$$\begin{aligned} \triangle N_A^2(k_y) &= \sum_{i,j \in A} \langle c_{i,k_y}^\dagger c_{j,k_y} \rangle \langle c_{j,k_y} c_{i,k_y}^\dagger \rangle \\ &= \mathrm{Tr}[\mathcal{C}(1 - \mathcal{C})] \ , \end{aligned} \qquad (12)$$

yielding $\triangle N_A^2(k_y) = \sum_i \zeta_i (1 - \zeta_i)$, which is in keeping with the variance formula of the Bernoulli distributions. It then follows that the variance is also dominated by the low-energy boundary excitations ($0 < \zeta_i < 1$). Moreover, each maximally entangled state with $\varepsilon_m = 0$ ($\zeta_m = 1/2$) contributes a maximal value to the subsystem particle number fluctuation and the EE, which cannot be eliminated by adiabatic continuous deformation.

In order to find a definite relationship between the EE and the variance, one can construct a concave function $f(x) = -\ln x/(1-x)$ for $x \in [0, 1]$, and apply the Jensen's inequality

$$-x \ln x - (1 - x) \ln(1 - x) \geqslant (4 \ln 2) \cdot x(1 - x) \ . \qquad (13)$$

The equality is taken if and only if $x = 1/2$. Equation (13) enables us to make a lower-bound estimation of the EE

$$s_{ent}(k_y) \geqslant (4 \ln 2) \cdot \triangle N_A^2(k_y) \ . \qquad (14)$$

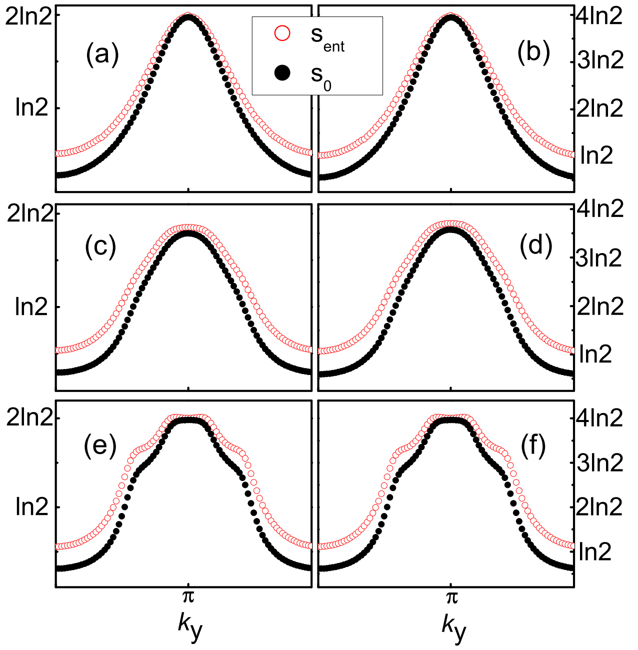

FIG. 5: (Color online) Entanglement entropy in comparison with subsystem particle number fluctuation for the QSH phase (upper row), the insulator phase (middle row), and the quantum anomalous Hall phase (lower row), in the cylinder geometry (left panels) and torus geometry (right panels). All the parameters are same as those in Fig. 2.

Thus a lower bound of the EE is given by $s_0(k_y) \equiv (4\ln 2)\cdot \triangle N_A^2(k_y)$, which is directly proportional to the particle number fluctuation of subsystem. In Fig. 5 we plot $s_{ent}(k_y)$ and $s_0(k_y)$ in the QSH phase, insulator phase, and quantum anomalous Hall phase. In all the cases, the curves for the particle number fluctuation behave somewhat similarly, and are very close to the corresponding EE. This similarity was observed in the nontopological systems lately[25], and here we find that the similarity remains to hold for the topologically nontrivial system.

Furthermore, one can use $N_A(k_y) = \sum_{i\in A} c^{\dagger}_{i,k_y} c_{i,k_y}$ to verify $\triangle N_A^2 = \sum_{k_y} \triangle N_A^2(k_y) \rightarrow \frac{L_y}{2\pi}\int dk_y N_A^2(k_y)$, indicating that $\triangle N_A^2(k_y)$ satisfies a area law[24], similar to the EE, $S_{ent} = \sum_{k_y} s_{ent}(k_y) \rightarrow \frac{L_y}{2\pi}\int dk_y s_{ent}(k_y)$. Therefore, the subsystem particle number fluctuation shares several common characteristics with the EE, and so can be utilized to detect the EE experimentally.

V. SUMMARY

To conclude, we have investigated the relationship between the quantum entanglement and subsystem particle number. The spin trace indices can reveal the topological invariants and be used to classify different phases in QSH systems. This new tool always works well even though s_z is not conserved. As to the subsystem particle number fluctuation, it shares several common properties with the EE. They both satisfy the same area law, and are dominated by the boundary excitations with each zero mode having a maximal contribution. The connection between the two quantities is universal, regardless of whether the system has a nontrivial band topology. As a result, the subsystem particle number fluctuation, as an observable quantity, can be used to detect the EE experimentally[25].

VI. ACKNOWLEDGMENTS

This work is supported by the State Key Program for Basic Researches of China under Grants Nos. 2009CB929504 (LS), 2011CB922103, and 2010CB923400 (DYX), the National Natural Science Foundation of China under Grant Nos. 11074110 (LS), 11074111 (RS), 11174125, 11074109, 91021003 (DYX), and a project funded by the PAPD of Jiangsu Higher Education Institutions.

---

[*] Electronic address: shengli@nju.edu.cn

[1] K.v. Klitzing, G. Dorda, and M. Pepper, Phys. Rev. Lett. **45**, 494 (1980).
[2] D.C. Tsui, H.L. Stormer, and A.C. Gossard, Phys. Rev. Lett. **48**, 1559 (1982).
[3] F.D.M. Haldane, Phys. Rev. Lett. **61**, 2015 (1988).
[4] D.J. Thouless, M. Kohmoto, M.P. Nightingale, and M.den. Nijs, Phys. Rev. Lett. **49**, 405 (1982).
[5] C.L. Kane and E.J. Mele, Phys. Rev. Lett. **95**, 226801 (2005).
[6] B.A. Bernevig, T.L. Hughes, and S.C. Zhang, Science **314**, 1757 (2006).
[7] M.Z. Hasan and C.L. Kane, Rev. Mod. Phys. **82**, 3045 (2010).
[8] X.L. Qi and S.C. Zhang, Physics Today. **63**, 33 (2010).
[9] C.L. Kane, and E.J. Mele, Phys. Rev. Lett. **95**, 146802 (2005).
[10] L. Sheng, D.N. Sheng, C.S. Ting, and F.D.M. Haldane, Phys. Rev. Lett. **95**, 136602 (2005); D.N. Sheng, Z.Y. Weng, L. Sheng, and F.D.M. Haldane, Phys. Rev. Lett. **97**, 036808 (2006).
[11] E. Prodan, Phys. Rev. B **80**, 125327 (2009); E. Prodan, New J. Phys. **12**, 065003 (2010).
[12] L. Amico, R. Fazio, A. Osterloh, and V. Vedral, Rev. Mod. Phys. **80**, 517 (2008); R. Horodecki, P. Horodecki, M. Horodecki, and K. Horodecki,Rev. Mod. Phys. **81**, 865 (2009).
[13] M. Levin and X.G Wen, Phys. Rev. Lett. **96**, 110405 (2006)

[14] A. Kitaev and J. Preskill, Phys. Rev. Lett. **96**, 110404 (2006).

[15] M. Haque, O. Zozulya, and K. Schoutens, Phys. Rev. Lett. **98**, 060401 (2007); O.S. Zozulya, M. Haque, K. Schoutens, and E.H. Rezayi, Phys. Rev. B **76**, 125310 (2007).

[16] X. Chen, Z.C. Gu, and X.G. Wen, Phys. Rev. B **83**, 035107 (2011); Z.X. Liu, M. Liu, X.G. Wen, Phys. Rev. B **84**, 075135 (2011).

[17] X.G. Wen, Quantum Field Theory Of Many-body Systems.(Oxford University Press, New York, 2004).

[18] H. Li and F.D.M. Haldane, Phys. Rev. Lett. **101**, 010504 (2008)

[19] A. Alexandradinata, T.L. Hughes, B.A. Bernevig, Phys. Rev. B. **84**, 195103 (2011).

[20] E. Prodan, T.L. Hughes, and B.A. Bernevig, Phys. Rev. Lett. **105**, 115501 (2010); H.Yao and X.L. Qi, Phys. Rev. Lett. **105**, 080501 (2010); T.L. Hughes, E. Prodan, and B.A. Bernevig, Phys. Rev. B **83**, 245132 (2011).

[21] L. Fidkowski, T.S. Jackson, and I. Klich, Phys. Rev. Lett. 107, 036601 (2011)

[22] Z. Qiao, S.A. Yang, W. Feng, W.K. Tse, J. Ding, Y. Yao, J. Wang, and Q. Niu, Phys. Rev. B **82**, 161414(R) (2010); Y.Y. Yang, Z. Xu, L. Sheng, B.G. Wang, D.Y. Xing, and D.N. Sheng, Phys. Rev. Lett. **107**, 066602 (2011).

[23] I. Peschel, J. Stat. Mech. (2004) P06004.

[24] J. Eisert, M. Cramer, and M.B. Plenio, Rev. Mod. Phys. **82**, 277 (2010).

[25] H.F. Song, C. Flindt, S. Rachel, I. Klich, and K.L. Hur, Phys. Rev. B. **83**, 161408(R) (2011); H.F. Song, S. Rachel, C. Flindt, I. Klich, N. Lafroncie, and Karyn and K.L. Hur, Phys. Rev. B. **85**, 035409 (2012).